The Journal of Experimental Biology 209, 1502-1515
Published by The Company of Biologists 2006
doi:10.1242/jeb.02146

Passive mechanical properties of legs from running insects

Daniel M. Dudek* and Robert J. Full
Department of Integrative Biology, University of California at Berkeley, Berkeley, CA 94720-3140, USA
*Author for correspondence (e-mail: dmdudek@berkeley.edu)

Accepted 6 February 2006

Summary

While the dynamics of running arthropods have been modeled as a spring-mass system, no such structures have been discovered that store and return energy during bouncing. The hindleg of the cockroach *Blaberus discoidalis* is a good candidate for a passive, vertical leg spring because its vertically oriented joint axes of rotation limit the possibility of active movements and contributions of muscle properties. We oscillated passive legs while measuring force to determine the leg's dynamic, mechanical properties. The relative dimensionless stiffness of an individual cockroach leg was equal to that estimated for a single leg of a biped or quadruped. Leg resilience ranged from 60 to 75%, affording the possibility that the leg could function as a spring to store and return the mechanical energy required to lift and accelerate the center of mass. Because hysteresis was independent of oscillation frequency, we rejected the use of a Voigt model – a simple spring in parallel with a viscous damper. A hysteretic damping model fit the cockroach leg force–displacement data over a wide range of frequencies and displacement using just two parameters. Rather than simply acting as a spring to minimize energy, we hypothesize that legs must manage both energy storage and absorption for rapid running to be most effective.

Key words: locomotion, biomechanics, modeling, *Blaberus discoidalis.*

Introduction

Running by legged arthropods is well modeled as a spring-mass system in both the sagittal and horizontal plane (Blickhan and Full, 1987; Full and Tu, 1990; Full and Tu, 1991; Schmitt and Holmes, 2000a; Schmitt and Holmes, 2000b). Three or four legs sum to function as a single, virtual leg-spring, appearing to bounce the animal's center of mass forward (Blickhan and Full, 1993). However, direct evidence of spring-like function in arthropod legs during rapid running is lacking. Arthropods rely on energy storage and power amplification by elastic structures during flight, sound generation, jumping and predatory strikes (for a review, see Gronenberg, 1996). Insect flight might be impossible in the absence of elastic structures that reside in the thoracic cuticle, resilin pads and the flight muscles themselves (Ellington, 1984; Weisfogh, 1973). Jumping locusts store energy in passive skeletal elements that include the bending of their tibial leg segment, the compression of elastomeric structures and the stretching of extensor tendons or apodemes (Bennet-Clark, 1975; Katz and Gosline, 1992). The legs of arthropods, such as locusts and spiders, have been shown to be highly resilient, storing and returning as much as 90% of the energy invested to deflect them (Blickhan, 1986; Katz and Gosline, 1992; Sensenig and Shultz, 2003). Dynamic oscillations of legs within the range of displacements and frequencies observed during running are needed to search for spring-like behavior.

In the present study, we determine the passive mechanical properties of the cockroach leg and examine the role they might play in managing energy during running. The deathhead cockroach, *Blaberus discoidalis*, has the dynamics of a spring-mass system during running, but the presence and location of spring-like elements remain a mystery (Blickhan and Full, 1993; Full and Tu, 1990). We selected cockroaches to simplify our search, because their legs have more vertically oriented joint axes such that a vertical displacement of a leg results in passive deflection of the exoskeleton rather than rotation of flexible joints under muscle control. Since the leg cuticle in other terrestrial insects is more than 90% resilient (Blickhan, 1986; Katz and Gosline, 1992; Sensenig and Shultz, 2003), we hypothesized that during running the leg acts as an energy-storing spring. Rapidly running cockroaches, cycling their legs at high frequencies, have little time to react to perturbations and yet these insects appear to absorb energy effectively and self-stabilize when perturbed. Jindrich and Full found that these cockroaches do not even require step transitions to recover from lateral perturbations caused by force impulses as high as 80% of forward running momentum (Jindrich and Full, 2002). Given their remarkable stability, we also hypothesize that legs act as energy-absorbing dampers, passively removing energy from perturbations, potentially simplifying control. By directly oscillating legs as we measured force, we tested whether an arthropod leg during running operates as a visco-

elastic structure represented by a simple spring in parallel with a viscous damper – often referred to as a Voigt model.

Materials and methods

Animals

Adult deathhead cockroaches (*Blaberus discoidalis* L.) of both sexes were obtained from Carolina Biological Supply (Gladstone, OR, USA) and used for all experiments (3.08±0.73 g, *N*=12 animals). Animals were housed in large plastic containers and fed dried dog food and water *ad libitum.* All cockroaches were euthanized immediately prior to an experiment in a 237-ml jar saturated with ethyl acetate vapor. Experiments were performed at room temperature (24°C).

Dynamic oscillations

Dynamic oscillations of the meta-thoracic limbs of cockroaches were performed to quantify their viscoelastic properties. Oscillations were performed on legs using two distinct preparations: one in which the body–coxa joint was rigidly fixed and another where the body–coxa joint was free to rotate. This was done in an attempt to bound the possible material properties of the leg from zero muscle activation (free-coxa) to infinitely stiff muscles (fixed-coxa). Since the joint axes of the more distal joints are oriented nearly vertical (Fig. 1A,B), muscle activation should have minimal effect on material properties during vertical oscillations.

In the fixed-coxa preparation (Fig. 1C), the ablated, meta-thoracic limb was affixed using epoxy resin to 0.95 cm-thick Plexiglas such that the trochanter, femur and tibia were free to rotate. Legs (*N*=7 animals, *n*=13 legs) were cut as proximally as possible in the unsclerotized region of the body–coxa joint using fine dissecting scissors and the tarsus was removed. No hemolymph loss was observed from either end of the leg. One end of a stainless steel pin (0.33 mm o.d.) was inserted into the distal tip of the tibia and secured with cyanoacrylate. The other end of the pin was attached to the arm of a servo-motor (300B-LR; Aurora Scientific, Aurora,

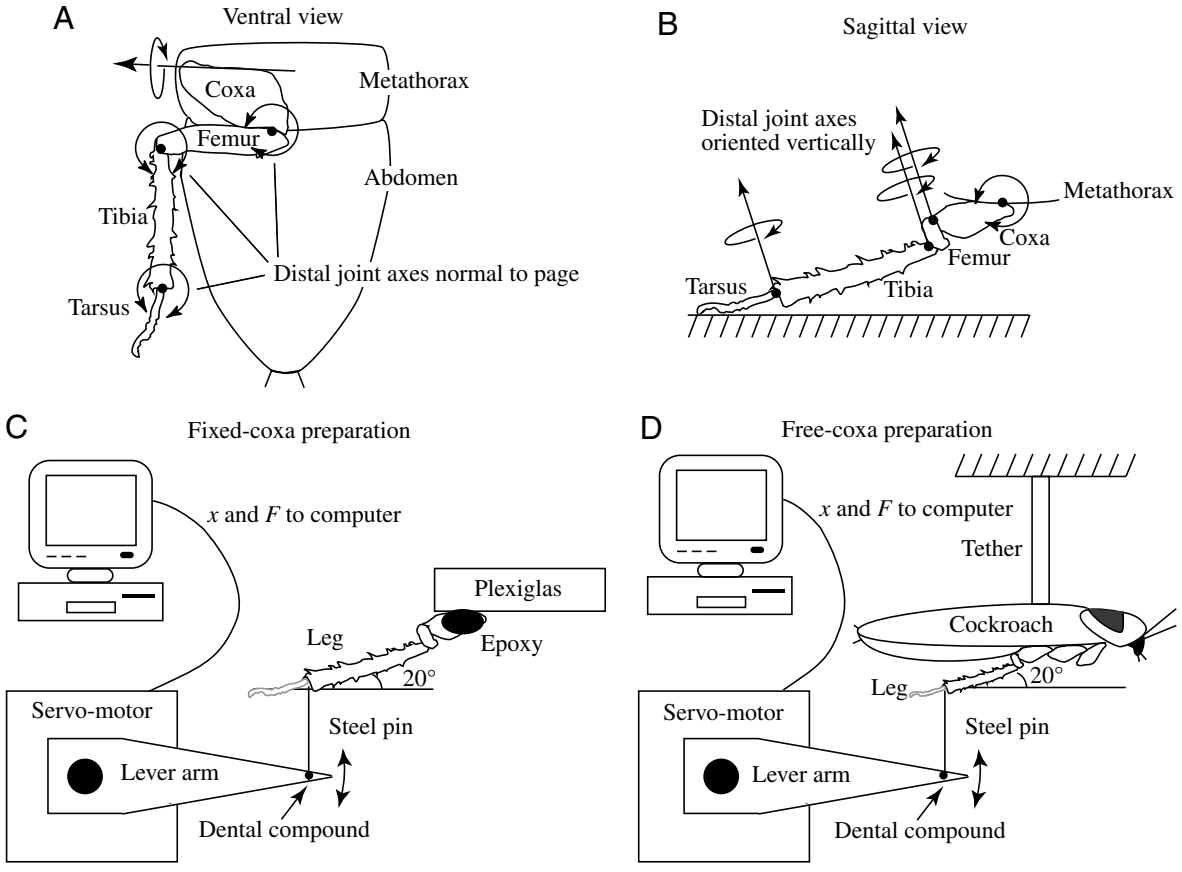

Fig. 1. The distal end of the tibia was attached to the arm of a servo-motor *via* a stainless steel pin. In both preparations, the angle between the steel pin and tibia was 110° because the body–coxa joint is held at a constant 20° during locomotion (Kram et al., 1997). The hindlimb was chosen due to its vertically oriented joint axes, where vertical deflections of the leg are absorbed by either the body–coxa joint or passive deflection of the exoskeleton. The servo-motor input sinusoidal oscillations from 0.01 to 100 Hz and 0.1 to 1.0 mm and recorded the induced forces. (A) Ventral view of the joint axes of rotation in the meta-thoracic leg. (B) Sagittal view of the joint axes of rotation in the meta-thoracic leg. (C) In the fixed-coxa preparation, the leg was removed and affixed with epoxy resin to 0.95 cm-thick Plexiglas. The tarsus (gray broken line) was removed. (D) In the free-coxa preparation, the cockroach was tethered to a bronze rod *via* the metanotum. These two preparations were chosen to bound the effect muscle activation at the body–coxa joint could have on leg properties. The tarsus (gray broken line) was removed.

ON, Canada) using dental compound (Kerr; Orange, CA, USA). The servo-motor input a time-varying displacement while simultaneously measuring force with a resolution of 0.25 mN.

In the free-coxa preparation (Fig. 1D), the euthanized cockroach was rigidly tethered to a bronze rod by the metanotum. The meta-thoracic limb (N=5 animals, n=10 legs) was attached to the arm of a servo-motor in the same manner as the fixed preparation. In this preparation, the body–coxa joint and all leg joints distal to it were free to rotate.

In both preparations, dynamic tests of the limb were performed in the dorso-ventral direction with sinusoidal displacements ranging from 0.1 to 1.0 mm at frequencies ranging from 0.05 to 60 Hz. The tibia and the pin connecting the limb to the servo-motor made a 110° angle relative to one another (Fig. 1C,D). The leg was oscillated dorso-ventrally to simulate the position of the legs and the effect of the body mass pushing down during the mid-stance of running. It also simulates a vertical perturbation of the leg during mid-swing. The displacements were chosen because the center of mass (COM) has been calculated to deflect vertically 0.3 mm during a stride (Full and Tu, 1990). The angle was chosen because the meta-thoracic body–coxa joint is held at a nearly constant 20° angle during the stance phase of running (Kram et al., 1997).

Controls

Preparation

To gain the most secure and repeatable connection, the lever was attached to the most distal portion of the tibia. Leaving the tarsus intact resulted in a 30 min delay between euthanasia and testing because of the need for the adhesive to dry. Removal of the tarsus decreased preparation to 5 min. For all data presented in this study, the tarsus of each tested leg was removed (Fig. 1C,D). As a control, we performed tests 30 min *post-mortem* without removing the tarsus. Results from legs with tarsi were not significantly different from legs without tarsi (P>0.05), where tests began 5 min *post-mortem*. Leg properties remained unchanged for at least 3 h in both the fixed-coxa and free-coxa preparations. Jensen and Weis-Fogh observed water loss in ablated locust tibia at a rate of 1% per hour, but '*48 h of storage without protection against evaporation had no appreciable effect upon the stress–strain relationship*' of cuticle ribbons (Jensen and Weis-Fogh, 1962). Therefore, if desiccation has an effect on material properties, it either occurs entirely in the first 5 min or requires more than 3 h to be measured.

Muscle activity

To test if *post-mortem* reflex muscle activity was playing a role in the legs of euthanized cockroaches, electromyograms were recorded from three coxa depressor muscles (177c, 177d and 179), one coxa levator (182c), one tibia extensor (194a) and one tibia flexor (185) (following Watson and Ritzmann, 1998). No muscle activity was observed in any of the six muscles examined.

Hemolymph pressure

While we did not measure internal pressure directly, it did not affect the mechanical properties of the leg. Removing the tarsus or cutting a hole in the mesonotum, both of which should eliminate internal leg pressure, had no significant effect. Moreover, hemolymph pressure in the cockroach *Periplaneta americana* has been shown to be only –0.005 atm (101.325 kPa atm^{-1}) (Davey and Treherne, 1964). While large fluctuations in hemolymph pressure have been observed during digging movements in newly emerged adult flies (from 0.05 atm at rest to as high as 0.15 atm), '*running merely produces a slight irregularity of the (pressure) traces*' (Cottrell, 1962). To test for pressure effects, we compared living cockroaches with euthanized cockroaches and found no significant difference. It is possible that the thorax depressurizes *post-mortem*, but the leg properties of living, recently actively struggling cockroaches were not different from those of living, calmly standing cockroaches.

Data acquisition and parameter calculations

Displacement and force signals from the servo-motor were digitized (board AT-MIO-16E-1; National Instruments, Austin, TX, USA) at sampling rates dependent on oscillation frequency and stored to the hard disk of a personal computer (Berta, Transduction Ltd, Mississauga, ON, Canada) running analysis software (MATLAB, The MathWorks, Natick, MA, USA).

Prior to any calculations, raw force and displacement signals were filtered using a 4th-order low-pass Butterworth filter at one-quarter the peak cutoff frequency for each trial. Peak cutoff frequency varied from trial to trial because oscillation frequency and sampling rate varied. For example, when sampling at 4000 Hz, the peak cutoff frequency to prevent aliasing is 2000 Hz, and one-quarter the peak cutoff frequency is 500 Hz. The maximum allowed frequency of the filter was never less than eight times the oscillation frequency. Visual inspection of the pre- and post-filtered power spectra did not reveal any noticeable structures outside the allowed frequency band. At low frequencies, spectral artifacts due to the intermittent movement of the lever arm were observed and removed by this filter. All calculations were performed using a mathematics program (MATLAB).

Impedance

Mechanical impedance (Z) or total dynamic stiffness (Wainwright et al., 1976) is the ratio of the greatest magnitude of a sinusoidally varying force to the greatest magnitude of a displacement. It has both a static component related to displacement and a dynamic component related to velocity and acceleration. Here, it represents the time-varying resistance of the limb to deformation and was calculated as:

$$Z = (F_{max} - F_{min}) / (x_{max} - x_{min}) , \quad (1)$$

where F is the force induced and x is the displacement measured per oscillation.

Phase shift

Phase shift (δ) for a paired force–displacement response is here defined as the angle between the maximum force and the maximum displacement. A measure of internal resistance (damping) is provided by tan(δ). We determined phase shift by dividing the time lag (t) between force and displacement peaks by the period of oscillation (T):

$$\delta = t / 2\pi T . \quad (2)$$

Resilience

Resilience (R) is the ratio of the energy recovered elastically to the energy input to the limb in each oscillation:

$$R = (E_{load} - E_{lost}) / E_{load} , \quad (3)$$

where E_{load} is the loading energy (area under the loading curve of the hysteresis loop) and E_{lost} is the energy lost per cycle, or hysteresis (area inside the hysteresis loop).

Modeling leg properties

Any model of the dynamic behavior of biomaterials must take into account both the in-phase (storage) and out-of-phase (loss) components of the induced force response. The most common approach taken in biology is to use a complex modulus (Wainwright et al., 1976), where the resultant stress (force per unit area), σ, of a material oscillated through a strain (normalized displacement), ϵ, is:

$$\sigma = E^*_{(\omega)}\epsilon , \quad (4)$$

where E^* is the complex modulus as a function of oscillation frequency, ω. To determine the in-phase and out-of-phase contributions, E^* can be broken into storage (E') and loss (E'') moduli:

$$E^* = E' + iE'' , \quad (5)$$

(i=$\sqrt{-1}$) and the phase shift is usually presented as its tangent:

$$\tan(\delta) = E''/E' . \quad (6)$$

Resilience can be calculated from tan(δ) using:

$$R = [e^{-\tan(\delta)}]\ 100 . \quad (7)$$

The expectation of how E', E'' and R vary with frequency depends on the viscoelastic model chosen to represent the material. While these models have traditionally been used to characterize the stress and strain relationships of isolated samples of biomaterials (Wainwright et al., 1976), we consider the leg as a structure that depends on forces (F) and displacements (x) and model it as a one-dimensional point mass.

Viscous damping model – Voigt model

The most common viscoelastic models used in biology assume combinations of linear springs and viscous dampers (Vincent, 1990; Wainwright et al., 1976). We modeled the leg as a linear spring in parallel with a viscous damper (commonly referred to as the Voigt model), where:

$$F = m\ddot{x} + c\dot{x} + k_v x , \quad (8)$$

where velocity ($\dot{x}$) and acceleration ($\ddot{x}$) are the first and second time derivatives of x. We did not include the inertial term in our analysis because it accounted for less than 5% of the force below 25 Hz. We calculated stiffness (k_v) and damping (c) coefficients by entering $F_{(t)}$, $x_{(t)}$ and $\dot{x}_{(t)}$ from oscillation trials into Eqn 8 and using a least squares minimization technique to find the best fit for k_v and c. When neglecting the inertial term in the Voigt model, E'=k_v, E''=$c\omega$, tan(δ)=$c\omega k_v^{-1}$ and $R \propto \omega^{-1}$.

Hysteretic damping model

Because of the lack of fit to a Voigt model, we calculated stiffness (k_h) and structural damping factor (γ) by fitting the force–displacement data to the hysteretic damping model (Nashif et al., 1985). The hysteretic damping model is also a linear model, but the damping is assumed to be structural instead of viscous. Rather than having a velocity-dependent damping term, both stiffness and damping are proportional to displacement where:

$$F = m\ddot{x} + (1 + i\gamma)k_h x , \quad (9)$$

where m is the mass of the leg and $\ddot{x}$ is the acceleration of the leg. In this case (and neglecting inertia), E'=k_h, E''=$k_h\gamma$, tan(δ)=γ and R is independent of oscillation frequency.

The hindlimb underwent a sinusoidal displacement oscillation of:

$$x = A \cos(\omega t) = \mathrm{Re}\,(Ae^{i\omega t}) , \quad (10)$$

where A is amplitude, t is time and RE indicates the real component. Replacing x in Eqn 9 with Eqn 10 and taking the real parts predicts that the resultant force in the leg as a function of time will be:

$$F_{(t)} = A\,[(k_h - \omega^2 m)\cos(\omega t) - \gamma k_h \sin(\omega t)] . \quad (11)$$

Stiffness and damping coefficients of the leg were determined by entering $F_{(t)}$, A, m and ω from oscillation trials into Eqn 11 and using a least-squares minimization technique to find the best fit for k_h and γ.

Statistical analysis

Both the left and right limbs were used from each animal tested. One-way analyses of variance (ANCOVAs) (separate slopes model) were performed to examine the relationship of the mechanical properties to the oscillation frequency. Data for the ANCOVAs were grouped by coxa preparation, amplitude of imposed displacement and, initially, left or right leg. Visual inspection showed that there was a break in the data at 25 Hz, with most properties increasing as a function of frequency up until 25 Hz and then remaining constant or decreasing as frequency increased further. Therefore, ANCOVAs were performed on two separate frequency ranges, 0.05–25 Hz and 25–60 Hz. Reported intercepts correspond to a frequency of 1 Hz because the ANCOVAs were performed on $\log_{10}$-transformed frequencies. All tests were performed using statistics software packages (JMP; SAS Institute, Cary, NC, USA; Statistics toolbox; The MathWorks). Unless otherwise stated, all reported values are

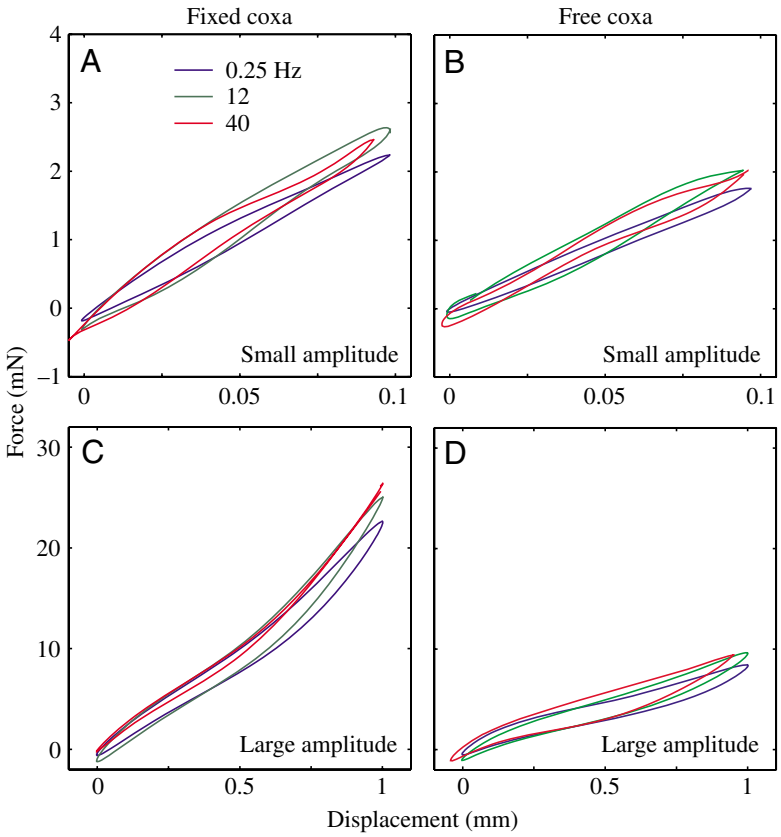

Fig. 2. Leg force as a function of displacement amplitude and oscillation frequency (blue line, 0.25 Hz; green line, 12 Hz; red line, 40 Hz). (A) Fixed coxa with small-amplitude oscillations (0.1 mm shown) resulted in nearly linear hysteresis loops. (B) Free coxa with small-amplitude oscillations (0.1 mm shown) showing near-linear hysteresis loops. (C) Fixed-coxa oscillations with large amplitudes exceeding 0.3 mm (1.0 mm shown) resulted in hysteresis loops with pronounced non-linearities. (D) Free-coxa oscillations with large amplitudes exceeding 0.3 mm showing non-linearities. The relatively larger areas of the loops in the free-coxa preparation (B,D) compared with the fixed-coxa legs (A,C) show the decreased resilience of a leg with a freely rotating coxa.

means ± standard errors (fixed-coxa, n=13 legs; free-coxa, n=10 legs).

Results

For each leg preparation, the left and right hindlimbs were tested with 85 treatments each for a total of 12 animals, 23 legs and 1955 tests. Tukey-Kramer *post-hoc* tests revealed that there was no significant difference in the mechanical properties of the left and right legs. Therefore, data from the left and right legs of each preparation were pooled for data analysis. Visual inspection revealed that the variance of the data for each individual was similar, so equal variances were assumed.

Induced forces

For all but the smallest amplitude displacement (0.1 mm), the resulting hysteresis loops were nonlinear (Fig. 2). The effect of increasing oscillation frequency on absolute forces was marginally significant, with induced force increasing less than 1 mN in most cases per decade increase of frequency from 0.05 to 25 Hz. Induced forces remained constant at frequencies from 25 to 60 Hz. Frequency did not have an effect on the shape of the hysteresis loops (Fig. 2). As displacement amplitude increased, the induced forces increased (ANCOVA with Tukey-Kramer honestly significant difference *post-hoc* test) and the loops became increasingly non-linear (Fig. 2C,D). At the same oscillation frequency and amplitude, induced forces were 50% (0.1 mm amplitude) to 65% (1.0 mm amplitude) lower (ANCOVA, Tukey-Kramer) for a leg with a freely rotating coxa when compared with a rigidly fixed leg. The percent difference between the two preparations was not a constant because the slopes of the regressions were significantly lower (ANCOVA, Tukey-Kramer) for the free-coxa preparation.

Average peak force ranged from 2.4±0.1 mN (0.1 mm at 0.25 Hz) to 21.9±2.2 mN (1.0 mm at 40 Hz) in the fixed-coxa leg. Forces of the free leg ranged from 1.2±0.1 mN (0.1 mm at 0.25 Hz) to 7.8±0.9 mN (1.0 mm at 40 Hz). By comparison, the vertical ground reaction force produced by the hindlimb during running is 11.9±0.9 mN (Full et al., 1991).

Impedance

Fixed-coxa leg impedance increased significantly as oscillation frequency increased from 0.05 to 25 Hz (Table 1) and declined slightly from 25 to 60 Hz (Fig. 3A). Increases in free-coxa leg impedance as a function of frequency (Fig. 3B) were significantly less pronounced (ANCOVA, Tukey-Kramer *post-hoc* test on slopes) than in the fixed-coxa preparation. For fixed-coxa legs, impedance was significantly greater for 0.1 mm oscillations than for the larger amplitudes (ANCOVA, Tukey-Kramer), with no significant difference for oscillations ranging from 0.3 to 1.0 mm. Free-coxa legs also had significantly higher impedance at low amplitude, but the intercepts continued to decrease as amplitude increased (Table 1). At the same oscillation frequency and amplitude, impedance was 50% (0.1 mm amplitude) to 65% (1.0 mm amplitude) lower (ANCOVA, Tukey-Kramer on intercepts) for a leg with a freely rotating coxa when compared with a rigidly fixed leg.

Phase shift

For both fixed- and free-coxa legs, the induced force reached a maximum prior to the maximum displacement, resulting in a phase shift, δ, between the force and displacement signals (Fig. 4A,B). There was no significant relationship between tan(δ) and oscillation frequency (ANCOVA, Tukey-Kramer).

Table 1. *One-way ANCOVA tables, separate slopes model testing the effect of oscillation amplitude on mechanical properties, with oscillation frequency as the covariate for either a fixed- or free-coxa leg*

		Fixed coxa			Free coxa		
Variable	Source	d.f.	*F*	*P*	d.f.	*F*	*P*
Impedance	Amplitude	4	4355.4	<0.0001	4	2874.1	<0.0001
	Frequency	1	6243.2	<0.0001	1	1794.0	<0.0001
	Amplitude × frequency	4	163.8	<0.0001	4	83.6	<0.0001
	Error	50			50		
Phase shift (δ)	Amplitude	4	9.9	<0.0001	4	4.2	0.0051
	Frequency	1	11.3	0.0015	1	17.2	0.0001
	Amplitude × frequency	4	0.6	0.6803	4	0.2	0.9210
	Error	50			50		
Hysteretic stiffness (*k*)	Amplitude	4	667.4	<0.0001	4	218.1	<0.0001
	Frequency	1	1191.3	<0.0001	1	291.3	<0.0001
	Amplitude × frequency	4	25.9	<0.0001	4	2.1	0.0958
	Error	50			50		
Damping factor (γ)	Amplitude	4	3.0	0.0295	4	1.7	0.1725
	Frequency	1	2.8	0.0998	1	0.1	0.7130
	Amplitude × frequency	4	0.1	0.9683	4	0.9	0.4605
	Error	45			45		

Frequency values were $\log_{10}$-transformed prior to statistical analysis.

Within the fixed- and free-coxa treatments, only the 0.1 mm amplitude oscillations had significantly different intercepts from the larger (0.3–1.0 mm) amplitude oscillations (Table 1; Fig. 4C,D). At the same oscillation frequency and amplitude, tan(δ) was the same at 0.1 mm amplitudes to 40% larger at 1.0 mm amplitudes (ANCOVA, Tukey-Kramer) in the free-coxa preparation compared with the fixed-coxa preparation.

Energy storage, return and lost

The work performed during each loading (E_{load}) and unloading cycle (E_{unload}) (see Fig. 4B) increased significantly, but only by a small percentage, with oscillation frequency from 0.05 to 25 Hz (Table 2; Fig. 5A,B). For both fixed- and free-coxa legs, energy expended per cycle increased significantly as oscillation amplitude increased (ANCOVA, Tukey-Kramer on intercepts). At the same oscillation frequency and amplitude, the loading and unloading (Table 2) energies in the free-coxa leg were 45% (0.1 mm amplitude) to 70% (1.0 mm amplitude) less (ANCOVA, Tukey-Kramer on intercepts) than the loading energies in the fixed-coxa leg.

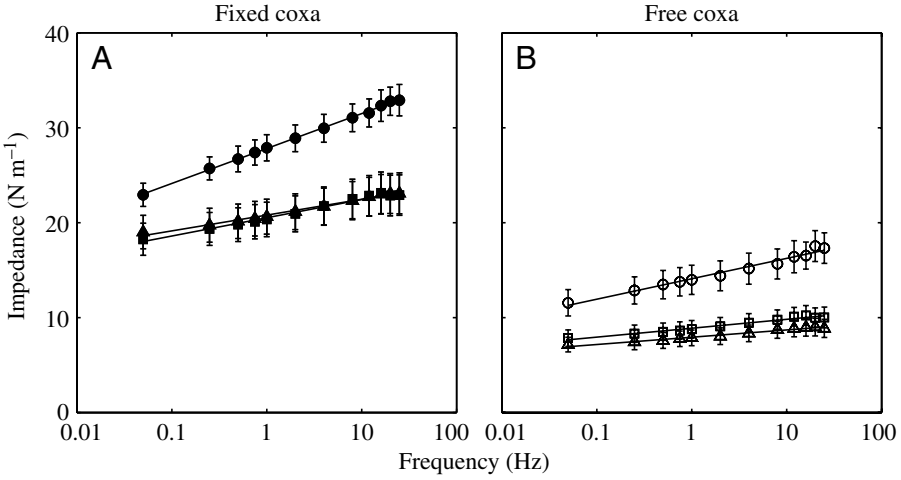

Fig. 3. Leg impedance as a function of frequency at amplitudes of 0.1 (circles), 0.5 (squares) and 1.0 mm (triangles). Leg impedance increased significantly as frequency increased from 0.05 to 25 Hz. Impedance of the fixed-coxa leg (A) was significantly greater than in the free-coxa leg (B).

For legs with a fixed coxa, the energy lost (E_{lost}) during each cycle actually decreased as oscillation frequency increased from 0.05 to 25 Hz (Table 2; Fig. 5E). However, this decrease was only statistically significant for 1.0 mm amplitude oscillations. For free-coxa legs, energy lost increased significantly, but only by a small percentage, for 0.5–1.0 mm amplitudes, as oscillation frequency increased (Fig. 5F). For both leg preparations, energy lost per cycle increased significantly as oscillation amplitude increased (ANCOVA, Tukey-Kramer on intercepts). At the same oscillation frequency and amplitude, the energy lost in the free-coxa leg was 50% (0.1 mm amplitude) to 25% (1.0 mm amplitude) less (ANCOVA, Tukey-Kramer on intercepts) than the energy lost in the fixed-coxa leg.

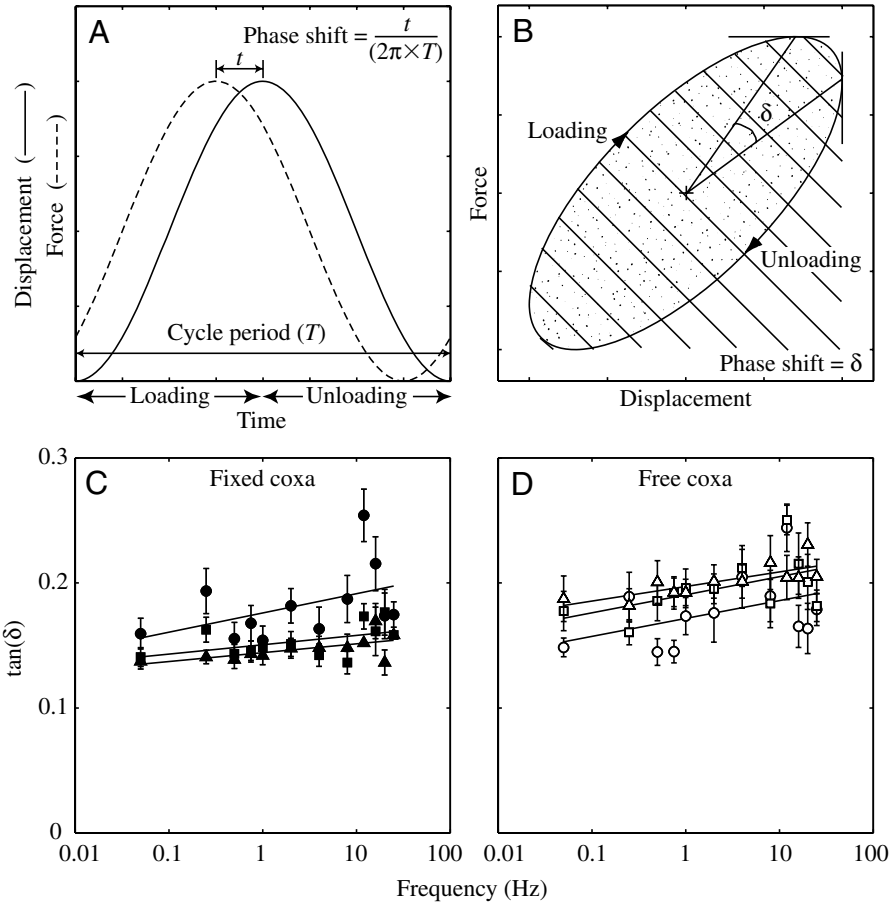

Fig. 4. Phase shift as a function of frequency at amplitudes of 0.1 (circles), 0.5 (squares) and 1.0 mm (triangles). (A) As the leg underwent deflection (solid line), the induced force (broken line) peak lagged behind the maximum displacement. (B) This phase shift, δ, can be seen as the angle between the maximum force and displacement of the hysteresis loop. Energy lost (E_{lost}) or hysteresis is shown in stipples. Energy of unloading ($E_{unloading}$) is shown as hatched. (C) In the fixed-coxa preparation, tan(δ) remained constant as frequency increased, and decreased as amplitude increased. (D) In the free-coxa preparation, tan(δ) remained constant as frequency increased, and increased as amplitude increased.

Table 2. *One-way ANCOVA tables, separate slopes model testing the effect of oscillation amplitude on leg energies (μJ) and resilience, with oscillation frequency as the covariate for either a fixed- or free-coxa leg*

		Fixed coxa			Free coxa		
Variable	Source	d.f.	*F*	*P*	d.f.	*F*	*P*
Loading energy	Amplitude	4	21915.5	<0.0001	4	20250.1	<0.0001
	Frequency	1	145.9	<0.0001	1	383.1	<0.0001
	Amplitude × frequency	4	20.4	<0.0001	4	67.7	<0.0001
	Error	50			50		
Unloading energy	Amplitude	4	17437.5	<0.0001	4	3770.5	<0.0001
	Frequency	1	341.0	<0.0001	1	58.8	<0.0001
	Amplitude × frequency	4	67.6	<0.0001	4	8.8	<0.0001
	Error	50			50		
Energy lost	Amplitude	4	1555.8	<0.0001	4	1523.7	<0.0001
	Frequency	1	15.1	<0.0001	1	39.0	<0.0001
	Amplitude × frequency	4	9.1	<0.0001	4	8.9	<0.0001
	Error	50			50		
Resilience	Amplitude	4	15.2	<0.0001	4	3.5	<0.0001
	Frequency	1	80.9	<0.0001	1	0.4	<0.0001
	Amplitude × frequency	4	1.3	0.2993	4	0.6	0.6847
	Error	50			50		

Frequency values were $\log_{10}$-transformed prior to statistical analysis.

Resilience

For both the fixed- and free-coxa preparations, resilience did not significantly increase with frequency, except at the largest (1.0 mm) amplitude (Table 2; Fig. 6A,B). In both preparations, the statistically significant slopes were small, ranging from 0.02 to 0.03. Resilience increased less than 3% per decade increase in oscillation frequency. The free-coxa leg was significantly less resilient than the fixed-coxa leg (ANCOVA, Tukey-Kramer on intercepts), averaging 71.7±0.6% for the fixed leg and 61.9±0.7% for the free leg (Fig. 6A,B).

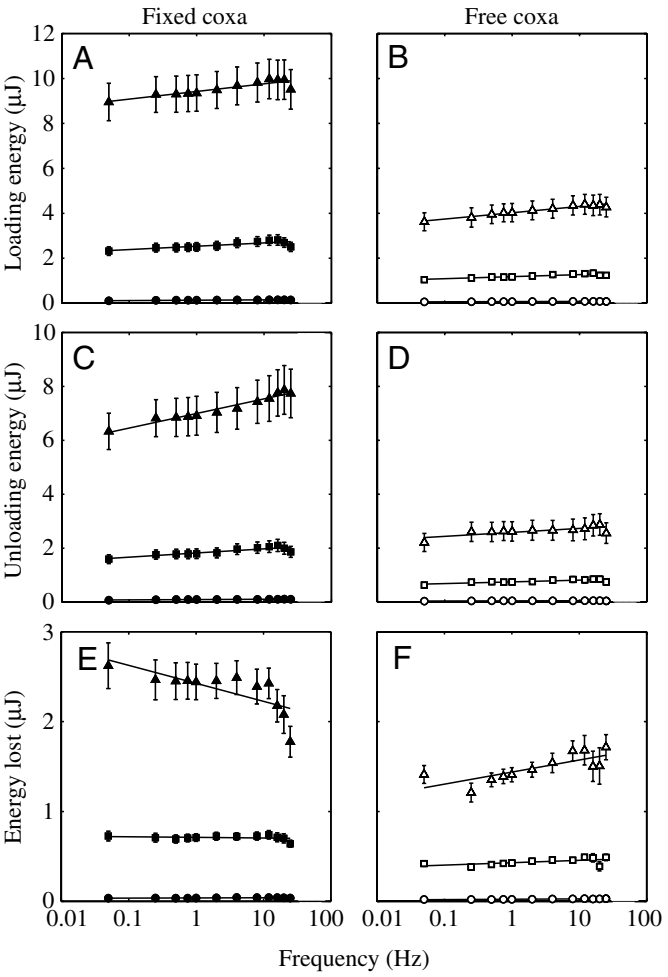

Fig. 5. Energy storage, returned and lost as a function of frequency at amplitudes of 0.1 (circles), 0.5 (squares) and 1.0 mm (triangles). (A) Loading energy in fixed coxa increased with increasing amplitude and as oscillation frequency increased from 0.05 to 25 Hz. (B) Loading energy in free coxa required 45–60% less energy than the fixed leg. (C) Unloading energy in the fixed coxa increased with increasing amplitude and as oscillation frequency increased to 25 Hz. (D) Unloading energy in the free coxa returned 50–70% less energy than the fixed leg. (E) Hysteresis (or lost energy) in the fixed-coxa preparation decreased as frequency increased, but was only significant at 1.0 mm oscillations. (F) Hysteresis in the free-coxa preparation increased as frequency increased significantly for 0.5 and 1.0 mm oscillations and was only about 30% less than the fixed-coxa legs.

Viscous damping model – Voigt model

The stiffness and damping parameters resulting from fitting the Voigt model to the data depend on both the frequency and amplitude of oscillation (Fig. 7). Legs with a fixed coxa were stiffer and more damped than those with a freely rotating coxa.

Leg stiffness increased as oscillation frequency increased

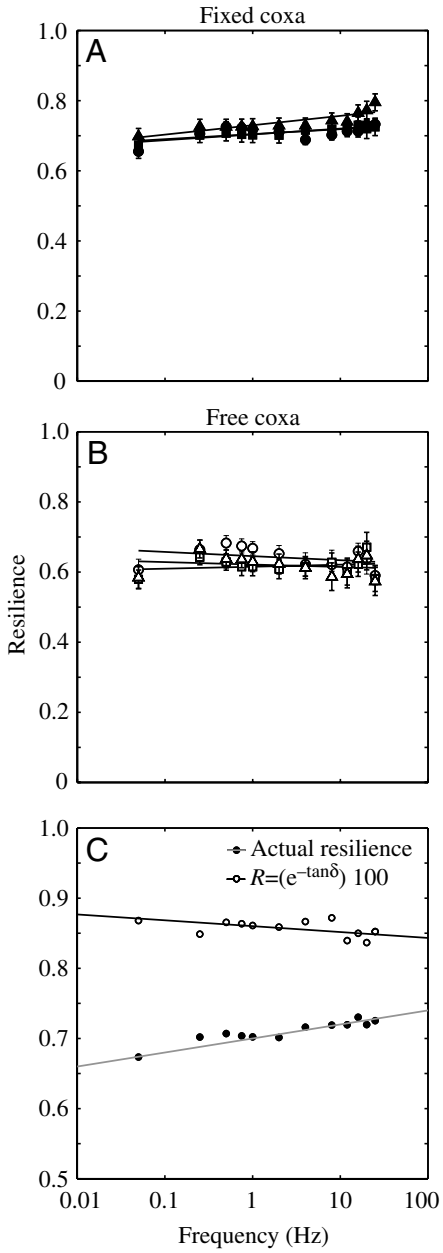

Fig. 6. Resilience (R) as a function of frequency at amplitudes of 0.1 (circles), 0.5 (squares) and 1.0 mm (triangles). (A) Fixed-coxa resilience was significantly greater than (B) free-coxa resilience. (C) Using tan(δ) to calculate resilience (black line and open circles) overestimates the actual values (gray line and filled circles) and produces an inverse dependence on frequency because the calculation is based on a linear model. While leg data are well fit by a linear model, the leg data are not linear, and care should be used when applying linear calculations to any biomaterial.

from 0.05 to 25 Hz (ANCOVA, Tukey-Kramer) but remained nearly constant from 25 to 60 Hz. Stiffness was significantly greater for 0.1 mm oscillations than for the larger amplitudes (ANCOVA, Tukey-Kramer) with no significant difference for oscillations ranging from 0.3 to 1.0 mm. At the same oscillation frequency and amplitude, stiffness was 50% (at 0.1 mm amplitude) to 60% (1.0 mm amplitude) lower (ANCOVA, Tukey-Kramer) for a leg with a freely rotating coxa when compared with a rigidly fixed leg (Fig. 7A,B).

The viscous damping coefficient was not constant. The coefficient decreased as both oscillation frequency and amplitude increased (ANCOVA, Tukey-Kramer; Fig. 7C,D). The damping coefficient for the free-coxa leg was 40% (at small amplitudes) to 50% (large amplitudes) smaller than the damping coefficient of the fixed-coxa leg.

Hysteretic damping model

For both the fixed- and free-coxa preparations, leg stiffness increased significantly (ANCOVA, Tukey-Kramer) as oscillation frequency increased from 0.05 to 25 Hz (Table 1; Fig. 8A,B) and continued to increase from 25 to 60 Hz. Stiffness was significantly greater for 0.1 mm oscillations than for the larger amplitudes (ANCOVA, Tukey-Kramer), with no significant difference for oscillations ranging from 0.3 to 1.0 mm. At the same oscillation frequency and amplitude, stiffness was 50% (at 0.1 mm amplitude) to 60% (1.0 mm amplitude) lower (ANCOVA, Tukey-Kramer) for a leg with a freely rotating coxa when compared with a rigidly fixed leg.

The structural damping factor of both the fixed- and free-coxa legs was independent of frequency and amplitude from 0.1 to 25 Hz (Table 1) and decreased from 40 to 60 Hz (Fig. 8C,D). The fixed-coxa leg was significantly less damped than the free-coxa leg (ANCOVA, Tukey-Kramer on intercepts), averaging 0.20±0.02 for the fixed leg and 0.28±0.02 for the free leg (Fig. 8C,D).

Hysteresis loops recreated using the stiffness and damping parameters resulting from fitting a damped spring (Eqn 11) to the data closely matched the actual data at low (0.1–0.3 mm) amplitudes (Fig. 9A). At the higher amplitude (0.5–1.0 mm) displacements, the linear lumped parameter model did not capture the nonlinearities in the leg data (Fig. 9B); however, the model's peak-to-peak displacement, force and area inside the loop were within 10% of the actual data.

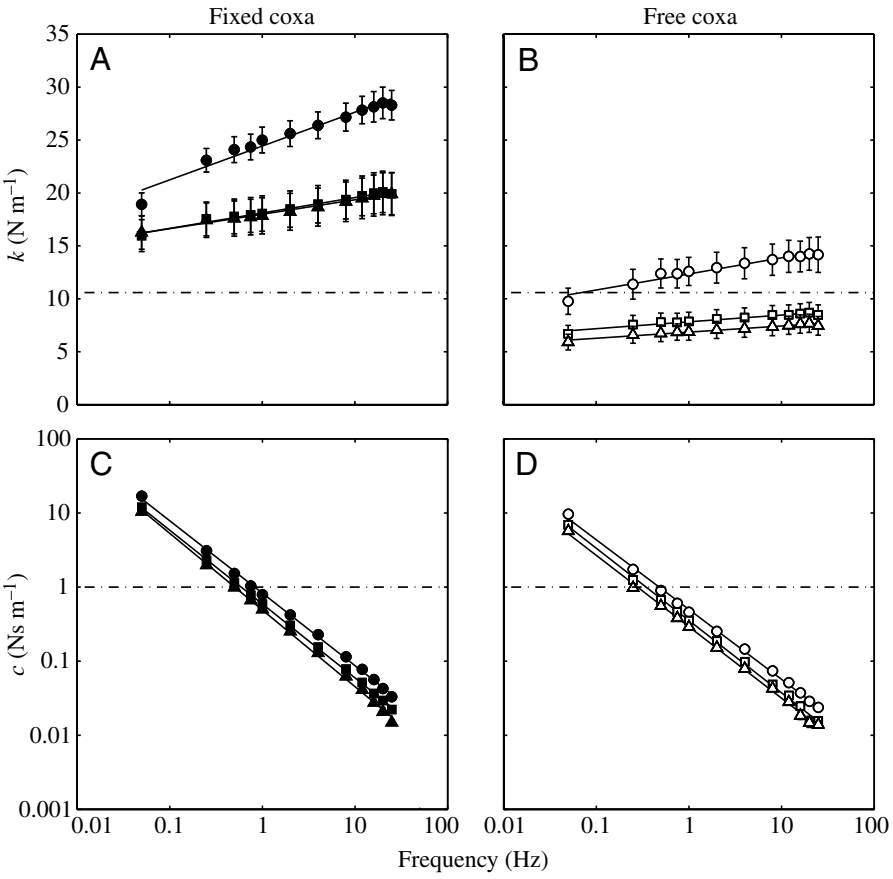

Fig. 7. Viscous damping model stiffness and damping coefficients as a function of frequency at amplitudes of 0.1 (circles), 0.5 (squares) and 1.0 mm (triangles). (A) Stiffness (k) of the fixed coxa. (B) Stiffness of the free-coxa leg. (C) Viscous damping coefficient (c) of the fixed-coxa leg decreased with oscillation frequency and amplitude. (D) Viscous damping coefficient of the free-coxa leg also decreased with frequency and amplitude. Viscous damping in the free-coxa leg was 40–50% less than in the fixed-coxa leg.

Discussion

Measured properties of cockroach legs did not fit a commonly applied spring-damper model but they did fit another simple, two-parameter model that captured the frequency independence of the hysteresis. While legs could function as springs during running, the damping present led us to suggest a view that energy management as it relates to stability and control best characterizes leg function rather than energy minimization.

Impedance and stiffness

Direct measurements of leg impedance (Fig. 3) and stiffness (Figs 7A,B, 9A,B) were similar to the best estimates derived from force-platform data (Full and Tu, 1990). Blickhan and Full calculated that one leg of a cockroach contributed 5.3 N m^{-1} to the stiffness of the SLIP (k_{SLIP}) (Blickhan and Full, 1993) or 15.9 N m^{-1} to the effective vertical stiffness [$k_{effvert}$; the ratio of the peak vertical force to the peak vertical displacement of the center of mass during the stance phase (McMahon and Cheng, 1990)]. We

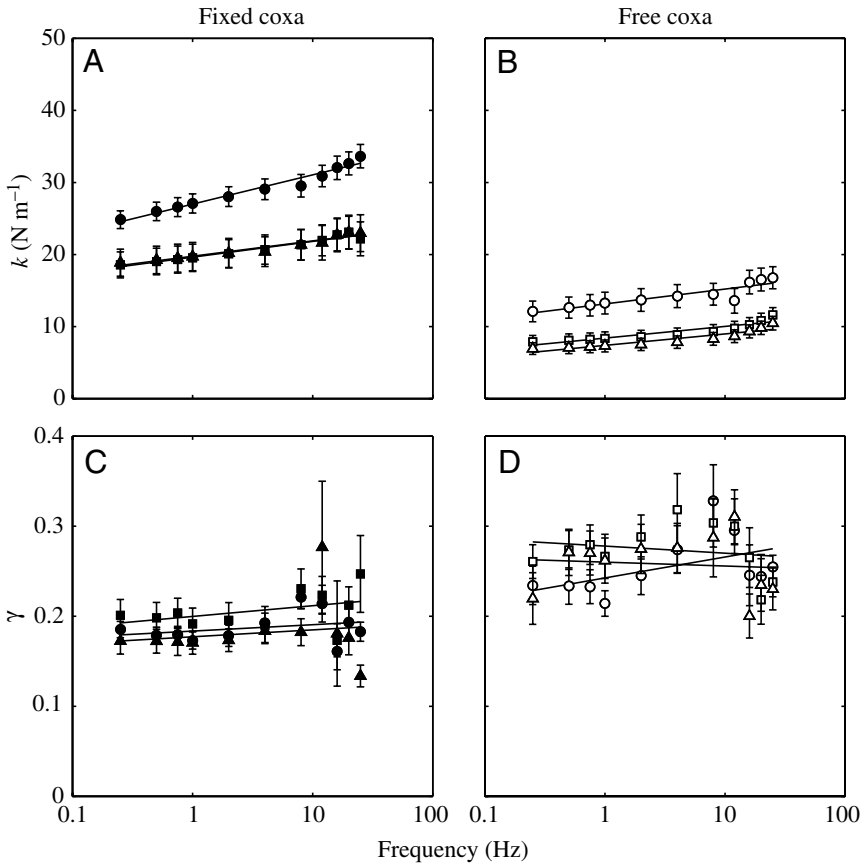

Fig. 8. Hysteretic damping model stiffness and damping coefficients as a function of frequency at amplitudes of 0.1 (circles), 0.5 (squares) and 1.0 mm (triangles). (A) Stiffness of the fixed-coxa leg increased with frequency from 0.05 to 25 Hz. The slopes and intercepts of the 0.3–1.0 mm amplitude oscillations were not significantly different from each other but were significantly lower than the 0.1 mm oscillations. (B) Stiffness of the free-coxa leg increased linearly with increasing frequency. As in the fixed-coxa preparation, the slopes and intercepts of the 0.3–1.0 mm amplitude oscillations were not significantly different from each other but were significantly lower than the 0.1 mm oscillations. The slopes and intercepts were 50–60% lower for the free-coxa leg than for the fixed-coxa leg. (C) Structural damping factor of the fixed-coxa leg was independent of oscillation frequency and amplitude. (D) Structural damping factor of the free-coxa leg also was independent of frequency and amplitude. Hysteretic damping in the fixed-coxa leg was 30% less than in the free-coxa leg.

predicted that our vertical loading regime would provide leg stiffness values that more closely matched $k_{effvert}$ than k_{SLIP}. Vertical leg stiffness values measured in the present study ranged from 9 N m^{-1} (free-leg) to 27 N m^{-1} (fixed-leg) (Fig. 9A,B) for cockroaches running at their preferred stride frequency (8 Hz) and with displacement amplitudes equal to the fluctuations of their center of mass (0.3 mm).

The similarity in measured and predicted leg stiffness values has several implications. First, it suggests that the exoskeleton may be a major contributor to leg stiffness. A detailed study of the coxa–body joint muscles and perhaps the femur reductor muscle at the trochanter–femur joint (Watson et al., 2002) is needed to test this assertion further, since we could only bound their function with a fixed- and free-coxa preparation. Second, the vertical loading regime for insects appears to yield reasonable estimates of leg stiffness. This may result from the fact that the relative compression of the SLIP in hexapedal runners is only one-third that observed in bipedal runners (Blickhan and Full, 1993). Hexapedal trotters also have far lower SLIP fore-aft ground reaction forces relative to vertical

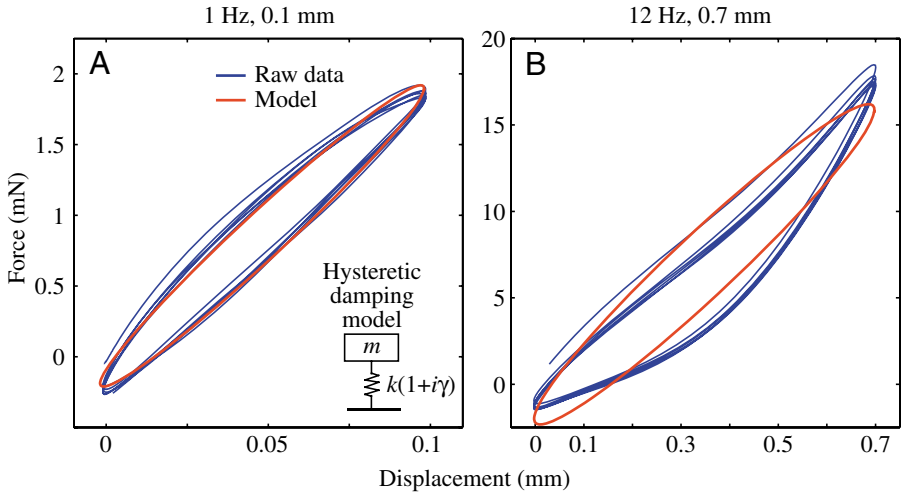

Fig. 9. Hysteretic damping model fitting. (A) Hysteresis loops recreated using the stiffness (k_h) and damping (γ) parameters from the hysteretic damping model fit (red line) closely matched the actual data (blue line) at low amplitudes. (B) Nonlinearities of the leg were not captured by the linear lumped parameter model, but the hysteretic model's peak-to-peak displacement, force and area inside the loop were within 10% of the actual data.

forces than do bipedal runners (Blickhan and Full, 1993). Third, the present leg stiffness data support the contention that hexapeds have a very stiff SLIP. Blickhan and Full found that the relative k_{SLIP} for hexapedal trotters, like cockroaches, was three times greater than values for bipedal runners and twice as great as quadrupedal trotters (Blickhan and Full, 1993). The relative stiffness of an individual cockroach leg reported here was equal to that estimated for a single leg of a biped or quadruped, despite the fact that insects appear to bounce off a tripod of legs each step (Blickhan and Full, 1993; Farley et al., 1993; Full and Tu, 1990).

The relatively high leg stiffness of hexapods may reveal a different strategy for the control of running compared with large bipeds and quadrupeds. The relatively high stiffness in hexapods results in small fluctuations of the center of mass. Preventing large fluctuations of the body may allow small, sprawled-posture animals to avoid contact with the substrate. The greater, relative k_{SLIP} in cockroaches results in higher relative frequencies that minimize falling time and increase the number of ground contacts to more quickly respond to perturbations or generate maneuvers.

Phase shift, energy and resilience

Resilience of the cockroach leg measured from cycle energies (Fig. 5) ranged from 0.6 in the free coxa to 0.75 in the fixed coxa (Fig. 6). These values are lower than that reported for isolated biological material known to participate in energy storage and return. Dynamic tensile tests of the plantaris tendon of sheep produced resilience values of 0.93 (Ker, 1981). Resilin, an elastomer involved in insect flight (Ellington, 1984; Weisfogh, 1973) and retraction of the cockroach tarsus during walking (Frazier et al., 1999; Neff et al., 2000) is 96–97% resilient (Gosline, 1980). Katz and Gosline calculated that the locust tibia used in jumping was more than 90% resilient (Katz and Gosline, 1992). Leg resilience values for the cockroach in the present study (Fig. 6) were more similar to those reported for arachnid joints that lack extensor muscles. Sensenig and Schultz showed that such joints with well-developed transarticular sclerites have resilience values from 70 to 90%, with the stored energy producing large enough torques to extend the joint during running (Sensenig and Schultz, 2003).

The resilience of cockroach legs was independent of frequency at all but the largest displacements (Fig. 6A,B; Table 2). At the largest amplitude oscillations, the increase was only 6% over two orders of magnitude in frequency. A similar resilience independence has been measured in sheep tendon from 1 to 11 Hz (Ker, 1981). The frequency independence of resilience in oscillating cockroach legs resulted from $E_{loading}$, $E_{unloading}$ and E_{lost} all changing little from 0.1 to over 20 Hz (Fig. 5). If cockroach legs function as a spring during locomotion, they would have the potential to return the same amount of energy at all running frequencies and speeds, all else being equal.

Calculating resilience using phase-shift (δ) equations (Eqns 6, 7; Fig. 4C,D) and the linear assumptions inherent in the complex modulus (E^*) over-estimated resilience by 23%, yielding values approaching 90% (Fig. 6C). Linear models assume perfect ellipsoids for force–displacement, hysteresis loops. Force–displacement data from cockroach legs became non-linear at displacements larger than 0.3 mm (Fig. 2C,D). The phase shifts of the raw data were less than that of the model, resulting in the substantial over-estimate of resilience (Fig. 6C). Linear models should be used cautiously with non-linear biomaterials. Whenever possible, resilience should be calculated by directly measuring force and displacement and using Eqn 3.

Hysteretic damping model

Force–displacement data from cockroach leg oscillations could not be modeled by a simple spring in parallel with a viscous damper (Eqn 4). We rejected the use of a Voigt model because no constant damping coefficient could be derived. Damping coefficient, c, varied by nearly four orders of magnitude over the range of frequencies tested (Fig. 7C,D). The Voigt model assumes that hysteresis or E_{lost} decreases as oscillation frequency increases. Hysteresis (Fig. 2) or E_{lost} (Fig. 5E,F) for the cockroach leg were independent of frequency or showed only a weak dependence on frequency at the larger displacements.

The dynamic properties of cockroach legs measured in the present study are not unusual. Many of the mechanical properties of the cockroach leg are characteristic of the majority of soft, biological tissues. The nonlinear, force–displacement relationship and the frequency independence of hysteresis are shared by muscles, arteries, veins, skin, tendon and collagen among other biological materials (Fung, 1984; Fung, 1993), as well as by human-made, rubber-based elastomers (Vincent, 1990). To better characterize the mechanical behavior of biomaterials, Fung proposed the use of the hysteretic damping model (Fung, 1967) that has a long history in analyzing vibration damping in airfoils (Fung, 1956), soils (Wolf, 1985), and elastomers (Nashif et al., 1985). The hysteretic damping model is so named because it was designed to reproduce the frequency independence of hysteresis or E_{lost} per cycle. Internal, material damping is considered dominant over viscous damping, so that damping is proportional to displacement. The model is simple and linear, possessing analytic solutions to sinusoidal, dynamic oscillations. Stiffness and damping coefficients are independent of frequency, so the behavior over a wide frequency range can be described using only two parameters. Additionally, there is little error introduced by integrating or differentiating the raw force or displacement data, since fitting the function (Eqn 11) requires only data that were directly measured.

The hysteretic damping model fits the cockroach leg force–displacement data over a wide range of frequencies and displacement using just two parameters, k_h and γ (Fig. 9). Because we determined k_h and γ using a least-squares method, the hysteresis loops recreated using the model coefficients captured, within 10%, the energies, resiliences and peak forces and displacements. Hysteretic leg stiffness increased

significantly as oscillation frequency increased from 0.05 to 25 Hz, but only by a small percentage (Table 1; Fig. 8A,B). The structural damping factor, γ, for both the fixed- and free-coxa legs was independent of frequency and amplitude from 0.1 to 25 Hz (Table 1; Fig. 8C,D).

Legs as energy-conserving springs during running

While the dynamics of small, running arthropods from cockroaches to crabs have been modeled as a spring-mass system, no elements have been discovered that store and return energy like a SLIP (Blickhan and Full, 1993; Sensenig and Shultz, 2003). The hindleg of the cockroach *B. discoidalis* is a candidate for an exoskeletal spring element due to its vertically oriented joint axes, which cause vertical ground reaction forces to passively bend the leg cuticle rather than a joint under muscle control. Given the material properties of the cockroach leg from the present study, we can estimate the extent to which the leg can function as an effective energy-conserving spring.

Running at 36 cm s^{-1} with a stride frequency of 12 Hz, a 2.5 g *B. discoidalis* generates a minimum of 32 μJ of external mechanical work per step to lift and accelerate its center of mass (calculated from figs 7 and 8 of Full and Tu, 1990). Dynamic oscillations at 12 Hz of the hindleg at the amplitude of the center of mass fluctuation (0.3 mm) induced leg forces of 6.91±0.58 mN with a stiffness of 10.98±1.03 N m^{-1} in the free-coxa preparation and 23.88±2.02 N m^{-1} in the fixed-coxa preparation (Fig. 8A,B). To determine the amount of mechanical energy that could be stored in a SLIP, we must first estimate its k_{SLIP}. Since we oscillated the leg vertically at an amplitude equal to the vertical deflection of the center of mass during running, we assumed that our leg stiffness values approximate $k_{effvert}$. We converted our values into k_{SLIP} using eqn 5 from Farley et al. (Farley et al., 1993), with a landing angle of 28.4°, a SLIP compression of 2 mm and a hip height of 12 mm. Blickhan and Full calculated that each of the three stance legs contributed a stiffness of 5.85 N m^{-1} to the k_{SLIP} of *B. discoidalis* (Blickhan and Full, 1993). Our estimated free-coxa k_{SLIP} for one leg was 3.15 N m^{-1}, whereas the fixed-coxa k_{SLIP} was 6.76 N m^{-1}, bounding Blickhan and Full's estimate (Blickhan and Full, 1993). The k_{SLIP} results from a support tripod and is therefore three times the single-leg k_{SLIP}, ranging from 9.45 to 20.28 N m^{-1} depending on the coxa preparation. The energy stored in a SLIP (E_{SLIP}) is:

$$E_{SLIP} = \tfrac{1}{2} k_{SLIP} (\Delta L)^2 , \quad (12)$$

where ΔL is the compression of the virtual leg spring [2 mm using eqn 3 from Blickhan and Full (Blickhan and Full, 1993)]. Using a k_{SLIP} for the free-coxa preparation, the energy stored in an undamped-SLIP is 20 μJ per step. Damping is present, however, with resilience values at approximately 66% (Fig. 6B). The damped-SLIP could therefore store and return 40% (13 out of 32 μJ) of the external mechanical work done to the center of mass each step. From this, we cannot reject the possibility that the hindleg of *B. discoidalis* operates as an energy-conserving spring during running.

Although our estimate of energy storage and return is similar to values for kangaroos (50%) (Alexander and Vernon, 1975), wallabies (25%) (Biewener and Baudinette, 1995) and humans (50%) (Ker et al., 1987), it should be considered, at best, as a first step towards determining the spring-like function of arthropod legs for a variety of reasons. First, our estimate of energy storage and return is almost certainly too high. The actual mechanical work done is likely to be much greater because the three legs of the support tripod do positive and negative work simultaneously as they push against one another (Donelan et al., 2002). Preliminary estimates of total mechanical work by integrating the instantaneous power at each joint over time result in values far exceeding the external work of the center of mass. We suspect future estimates of energy conservation to be closer to kangaroo rats (8%) (Biewener et al., 1981) than kangaroos. Second, even though each leg of an insect generates the same magnitude of vertical ground reaction force, horizontal forces differ along with leg morphology and orientation (Full et al., 1991). Studies directly measuring SLIP function during running with natural loading of the legs need to be conducted given the encouraging results of the present study. Third, we took advantage of the hindleg's greater dependence on passive structures, but future studies of the middle and front legs will require a greater understanding of muscle–apodeme function. Our simplifying assumption that all leg pairs contribute equally to spring-like function is unlikely to be verified.

Damping, stability and energy management

By their very name, spring-mass models of legged terrestrial locomotion have been biased towards spring-like energy conservation. Yet, here we report direct measurements of energy in oscillating cockroach legs that show the possibility of substantial damping even in skeletal structures (Figs 5, 6). We must remember that while the center of mass acts as if it were a SLIP during running, the same behavior could result in the absence of elastic structures where energy is lost to damping in the first half of the step, but then added in the second half of the step by way of muscle activation (Alexander, 1988). Surprisingly, human runners still use movement patterns that resemble a spring-mass system even when they must perform extra mechanical work on sand (Lejeune et al., 1998). Moritz and Farley discovered that human legs do not behave like springs during hopping on damped surfaces, yet their center of mass follows the same bouncing trajectory as if they were on an elastic surface (Moritz and Farley, 2003). These data do not support the view that animals use bouncing gaits solely because legs are energy-conserving springs.

The primary role of arthropod legs during running may not be energy storage and return. Full and Koditschek have argued (Full and Koditschek, 1999) that energy management resulting in stable locomotion is as important as energy minimization (Alexander, 1988; Cavagna et al., 1977). Ting et al. demonstrated that dynamic stability was required to explain rapid running in insects (Ting et al., 1994). Using a feed-forward, hexapod model, Kubow and Full showed that cockroach locomotion viewed in the horizontal plane could be

dynamically self-stabilizing with control algorithms essentially embedded in the mechanical system (Kubow and Full, 1999). Velocity perturbations alter the translation and/or rotation of the body, thereby providing 'mechanical feedback' through alterations in leg moment arms. With their simple lateral leg spring model, Schmitt and Holmes showed that passive mechanics of a spring-mass system locomoting forward by bouncing from side to side can provide asymptotic stability in body rotation and orientation following a lateral perturbation (Schmitt and Holmes, 2000a; Schmitt and Holmes, 2000b). With the addition of energy absorption, the lateral leg spring model becomes asymptotically stable with respect to velocity (Schmitt and Holmes, 2003). Estimating model parameters, such as mass, leg spring stiffness, leg angle, leg length and inertia, for the cockroach *B. discoidalis* reveals that animals operate at or near the stability optimum for each parameter (Schmitt et al., 2002). Spring-like center-of-mass trajectories may simplify the control of locomotion.

Finally, limbs do not only function during stance but must swing back to their anterior position to support the next step. The mechanical properties that manage energy could be critical if a leg gets perturbed when in the air. While contributing to energetic inefficiency, damping may play an important role in simplifying neural control and rejecting external perturbations. Feedback control using reflexes works best given high loop gains and little delay (Rack, 1981), but this situation is rarely seen in rapidly moving animals. Due to reflex delays during both conduction and muscle activation/force generation, the immediate response of a leg to an external perturbation, such as rough terrain or debris, may depend solely on its passive mechanical properties (Brown and Loeb, 2000; McMahon and Greene, 1979; Rack, 1981). This '*zero delay, intrinsic response of a neuromuscular-skeletal system to a perturbation*' that can act before reflexes has been termed a 'preflex' (Brown and Loeb, 2000).

Taken together, these studies support the hypothesis that tuned musculo-skeletal structures, such as legs, must manage energy for rapid running to be most effective.

We thank Lisa Pruitt, Francisco Velero-Cuevas, Benson Tongue, Mark Cutkosky and two anonymous reviewers for making helpful comments on earlier versions of this manuscript. This work was supported by DARPA/ONR – N00014-98-1-0747, DARPA/SPAWAR N66001-03-C-8045 and NSF EF 0425878 FIBR to R.J.F. and a Department of Integrative Biology summer research grant to D.M.D.

References

Alexander, R. McN. (1988). *Elastic Mechanisms in Animal Movement*. Cambridge: Cambridge University Press.

Alexander, R. McN. and Vernon, A. (1975). Mechanics of hopping by kangaroos (Macropodidae). *J. Zool. (Lond.)* **177**, 265-303.

Bennet-Clark, H. C. (1975). Energetics of jump of locust *Schistocerca gregaria*. *J. Exp. Biol.* **63**, 53-83.

Biewener, A. A. and Baudinette, R. V. (1995). *In vivo* muscle force and elastic energy storage during steady-speed hopping of Tammar wallabies (*Macropus eugenii*). *J. Exp. Biol.* **198**, 1829-1841.

Biewener, A., Alexander, R. M. and Heglund, N. C. (1981). Elastic energy storage in the hopping of kangaroo rats (*Dypodomys spectabilis*). *J. Zool. Lond.* **195**, 369-383.

Blickhan, R. (1986). Stiffness of an arthropod leg joint. *J. Biomech.* **19**, 375-384.

Blickhan, R. and Full, R. J. (1987). Locomotion energetics of the ghost crab. 2. Mechanics of the center of mass during walking and running. *J. Exp. Biol.* **130**, 155-174.

Blickhan, R. and Full, R. J. (1993). Similarity in multilegged locomotion: bounding like a monopode. *J. Comp. Physiol. A* **173**, 509-517.

Brown, I. E. and Loeb, G. E. (2000). A reductionist approach to creating and using neuromusculoskeletal models. In *Biomechanics and Neural Control of Posture and Movement* (ed. J. A. Winters and P. E. Crago), pp. 148-163. New York: Springer.

Cavagna, G. A., Heglund, N. C. and Taylor, C. R. (1977). Mechanical work in terrestrial locomotion – 2 basic mechanisms for minimizing energy expenditure. *Am. J. Physiol.* **233**, R243-R261.

Cottrell, C. B. (1962). Imaginal ecdysis of blowflies – observations on hydrostatic mechanisms involved in digging and expansion. *J. Exp. Biol.* **39**, 431-448.

Davey, K. G. and Treherne, J. E. (1964). Studies on crop function in cockroach (*Periplaneta americana* L). 3. Pressure changes during feeding + crop-emptying. *J. Exp. Biol.* **41**, 513-524.

Donelan, J. M., Kram, R. and Kuo, A. D. (2002). Simultaneous positive and negative external mechanical work in human walking. *J. Biomech.* **35**, 117-124.

Ellington, C. P. (1984). The aerodynamics of hovering insect flight. VI. Lift and power requirements. *Philos. Trans. R. Soc. Lond. B Biol. Sci.* **305**, 145-181.

Farley, C. T., Glasheen, J. and McMahon, T. A. (1993). Running springs – speed and animal size. *J. Exp. Biol.* **185**, 71-86.

Frazier, S. F., Larsen, G. S., Neff, D., Quimby, L., Carney, M., DiCaprio, R. A. and Zill, S. N. (1999). Elasticity and movements of the cockroach tarsus in walking. *J. Comp. Physiol. A* **185**, 157-172.

Full, R. J. and Koditschek, D. E. (1999). Templates and anchors: neuromechanical hypotheses of legged locomotion on land. *J. Exp. Biol.* **202**, 3325-3332.

Full, R. J. and Tu, M. S. (1990). Mechanics of six-legged runners. *J. Exp. Biol.* **148**, 129-146.

Full, R. J. and Tu, M. S. (1991). Mechanics of a rapid running insect: two-, four- and six-legged locomotion. *J. Exp. Biol.* **156**, 215-232.

Full, R. J., Blickhan, R. and Ting, L. H. (1991). Leg design in hexapedal runners. *J. Exp. Biol.* **158**, 369-390.

Fung, Y. (1967). Elasticity of soft tissues in simple elongation. *Am. J. Physiol.* **213**, 1532-1544.

Fung, Y. C. (1956). *An Introduction to the Theory of Elasticity*. New York: Wiley.

Fung, Y. C. (1984). Structure and stress–strain relationship of soft tissues. *Am. Zool.* **24**, 13-22.

Fung, Y. C. (1993). *Biomechanics: Mechanical Properties of Living Tissues*. New York: Springer-Verlag.

Gosline, J. M. (1980). The elastic properties of rubber-like proteins and highly extensible tissues. In *The Mechanical Properties of Biological Materials*, vol. 34 (ed. J. F. V. Vincent and J. D. Currey), pp. 331-357. Cambridge: Symposia of the Society for Experimental Biology/Cambridge University Press.

Gronenberg, W. (1996). Fast actions in small animals: springs and click mechanisms. *J. Comp. Physiol. A* **178**, 727-734.

Jensen, M. and Weis-Fogh, T. (1962). Biology and physics of locust flight. V. Strength and elasticity of locust cuticle. *Philos. Trans. R. Soc. Lond. B Biol. Sci.* **245**, 137-169.

Jindrich, D. L. and Full, R. J. (2002). Dynamic stabilization of rapid hexapedal locomotion. *J. Exp. Biol.* **205**, 2803-2823.

Katz, S. L. and Gosline, J. M. (1992). Ontogenic scaling and mechanical-behavior of the tibiae of the African desert locust (*Schistocerca gregaria*). *J. Exp. Biol.* **168**, 125-150.

Ker, R. F. (1981). Dynamic tensile properties of the plantaris tendon of sheep (*Ovis aries*). *J. Exp. Biol.* **93**, 283-302.

Ker, R. F., Bennett, M. B., Bibby, S. R., Kester, R. C. and Alexander, R. McN. (1987). The spring in the arch of the human foot. *Nature* **325**, 147-149.

Kram, R., Wong, B. and Full, R. J. (1997). Three-dimensional kinematics and limb kinetic energy of running cockroaches. *J. Exp. Biol.* **200**, 1919-1929.

Kubow, T. M. and Full, R. J. (1999). The role of the mechanical system in control: a hypothesis of self-stabilization in hexapedal runners. *Philos. Trans. R. Soc. Lond. B Biol. Sci.* **354**, 849-861.

Lejeune, T., Willems, P. and Heglund, N. C. (1998). Mechanics and energetics of human locomotion on sand. *J. Exp. Biol.* **201**, 2071-2080.
McMahon, T. A. and Cheng, G. C. (1990). The mechanics of running – how does stiffness couple with speed. *J. Biomech.* **23**, 65-78.
McMahon, T. A. and Greene, P. R. (1979). Influence of track compliance on running. *J. Biomech.* **12**, 893-904.
Moritz, C. T. and Farley, C. T. (2003). Human hopping on damped surfaces: strategies for adjusting leg mechanics. *Proc. R. Soc. Lond. B Biol. Sci.* **270**, 1741-1746.
Nashif, A., Jones, D. and Henderson, J. (1985). *Vibration Damping*. New York: John Wiley & Sons.
Neff, D., Frazier, S. F., Quimby, L., Wang, R. T. and Zill, S. (2000). Identification of resilin in the leg of cockroach, *Periplaneta americana*: confirmation by a simple method using pH dependence of UV fluorescence. *Arthropod Struct. Dev.* **29**, 75-83.
Rack, P. M. H. (1981). Limitations of somatosensory feedback in control of posture and movement. In *Handbook of Physiology, Section 1, The Nervous System*, *Vol. II, Parts 1 and 2, Motor Control* (ed. V. B. Brooks), pp. 229-256. Bethesda: The American Physiological Society.
Schmitt, J. and Holmes, P. (2000a). Mechanical models for insect locomotion: dynamics and stability in the horizontal plane – II. Application. *Biol. Cybern.* **83**, 517-527.
Schmitt, J. and Holmes, P. (2000b). Mechanical models for insect locomotion: dynamics and stability in the horizontal plane I. Theory. *Biol. Cybern.* **83**, 501-515.
Schmitt, J. and Holmes, P. (2003). Mechanical models for insect locomotion: active muscles and energy losses. *Biol. Cybern.* **89**, 43-55.
Schmitt, J., Garcia, M., Razo, R. C., Holmes, P. and Full, R. J. (2002). Dynamics and stability of legged locomotion in the horizontal plane: a test case using insects. *Biol. Cybern.* **86**, 343-353.
Sensenig, A. T. and Shultz, J. W. (2003). Mechanics of cuticular elastic energy storage in leg joints lacking extensor muscles in arachnids. *J. Exp. Biol.* **206**, 771-784.
Ting, L. H., Blickhan, R. and Full, R. J. (1994). Dynamic and static stability in hexapedal runners. *J. Exp. Biol.* **197**, 251-269.
Vincent, J. F. V. (1990). *Structural Biomaterials*. Princeton: Princeton University Press.
Wainwright, S. A., Biggs, W. D., Currey, J. D. and Gosline, J. M. (1976). *Mechanical Design in Organisms*. Princeton: Princeton University Press.
Watson, J. T. and Ritzmann, R. E. (1998). Leg kinematics and muscle activity during treadmill running in the cockroach, *Blaberus discoidalis*. I. Slow running. *J. Comp. Physiol. A* **182**, 11-22.
Watson, J. T., Ritzmann, R. E., Zill, S. N. and Pollack, A. J. (2002). Control of obstacle climbing in the cockroach, Blaberus discoidalis. I. Kinematics. *J. Comp. Physiol. A* **188**, 39-53.
Weisfogh, T. (1973). Quick estimates of flight fitness in hovering animals, including novel mechanisms for lift production. *J. Exp. Biol.* **59**, 169-230.
Wolf, J. P. (1985). *Dynamic Soil Structure Interaction*. New Jersey: Prentice Hall.